Inorganic Chemistry

Article

pubs.acs.org/IC

Bismuth–Halide Oxidative Addition and Bismuth–Carbon Reductive Elimination in Platinum Complexes Containing Chelating Diphosphine Ligands

S. Masoud Nabavizadeh,*[,†] Fatemeh Niroomand Hosseini,*[,‡] Negar Nejabat,[†] and Zahra Parsa[†]

[†]Department of Chemistry, College of Sciences, Shiraz University, Shiraz 71467-13565, Iran

[‡]Department of Chemistry, Shiraz Branch, Islamic Azad University, Shiraz 71993-37635, Iran

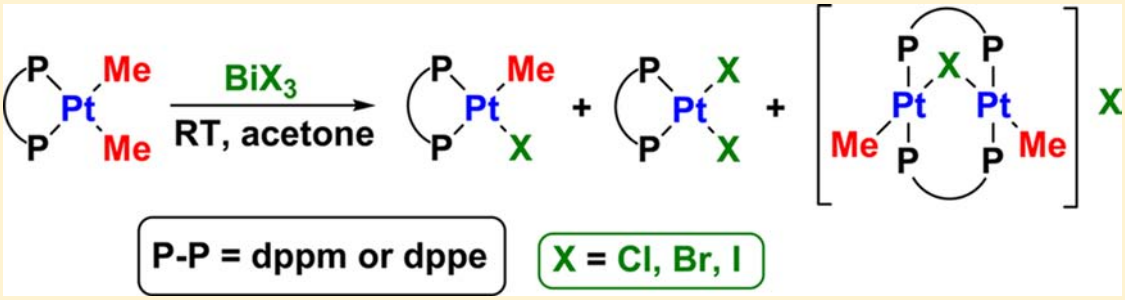

ABSTRACT: Reaction of BiX_3 (X = Cl, Br, I) with $[PtMe_2(P–P)]$, (**1a**, P–P = dppm; **1b**, P–P = dppe), occurs easily to yield a mixture of platinum(II) complexes $[PtMeX(P–P)]$, **2**, and $[PtX_2(P–P)]$, **3**, and the binuclear complex $[Pt_2Me_2(\mu\text{-}X)(\mu\text{-}dppm)_2]X$, **4**. On the basis of ^{31}P NMR and UV–vis spectroscopy, a mechanism is proposed in which the rate determining step is conversion of the yellowish Pt(II)-BiX_3 adduct $BiI_3{\cdot}[PtMe_2(dppm)]$, **A**, into the Pt(IV)–Bi(III) intermediate $[PtMe_2(BiX_2)\text{-}X(P–P)]$, **IM1**. Density functional theory (DFT) studies suggest that intermediate **IM1** may be formed in acetone solution which undergoes the Bi–C reductive elimination process before formation of complexes **2** and **3**. The structures of intermediates **IM1** were theoretically determined using DFT calculations. In dilute acetone solution, as monitored by UV–vis spectroscopy, the oxidative addition processes follow first order kinetics. The overall reaction is slower for heavier halide.

INTRODUCTION

Oxidative addition reaction of different polar and nonpolar reagents to transition metal complexes has been extensively investigated and is considered as a key step in many catalytically important chemical processes.[1] In particular, the related reactions involving Pt complexes with a wide variety of reagents have been studied in detail.[2] Oxidative addition of heavy metal compounds to transition metal complexes has also been investigated, and the addition of reagents including Sn–X, Hg–X, Te–X, and Ge–X bonds (X = halogen), to electron rich platinum(II) centers have been reported.[3] Besides, Braunschweig and co-workers have recently reported the oxidative addition of the bismuth-chloride bond to a Pt(0) complex.[4] As such, the $BiCl_3$ reagent acts as a Lewis-acid because of the relativistic contraction of the valence 6s Bi AO,[5] and the nucleophilic Pt(0) center in the first place attacks the Bi–Cl σ^*-orbital.[4]

On the other hand, reductive elimination reactions are among the most fundamental organometallic processes. In contrast to many reports on reductive elimination of R–R, R–H, Ar–Ar, and C–X,[6] on the basis of our knowledge, no studies on reductive elimination of Bi–C bonds from Pt(IV) complexes have been reported, although organobismuth compounds are useful in organic synthesis because of mild Lewis acidity, low toxicity, air stability, low cost, and ease of handling.[7]

In continuation of our interest in the investigation of oxidative addition reactions of different types of reagents to organoplatinum complexes,[8] in the present work, we have studied the reactions of platinum(II) complexes $[PtMe_2(P–P)]$, **1**, in which P–P = 1,1–bis(diphenylphosphino)methane (dppm) or 1,2-bis(diphenylphosphino)ethane (dppe), with bismuth trihalides, BiX_3 (X = Cl, Br, I). This seems to be the first example of bismuth–halide oxidative addition to organoplatinum(II) complexes and bismuth–carbon reductive elimination from Pt(IV) complexes.

EXPERIMENTAL SECTION

The NMR spectra were recorded as $CDCl_3$ or acetone-d_6 solutions on a Bruker Avance DRX 500 MHz spectrometer. The operating frequencies and references, respectively, are shown in parentheses as follows: ^1H (500 MHz, TMS) and ^{31}P (202 MHz, 85% H_3PO_4). All the chemical shifts and coupling constants are given in units of ppm and Hz, respectively. The absorption spectra and kinetic studies were measured using a Perkin–Elmer Lambda 25 UV–vis spectrometer with temperature control using an EYELA NCB–3100 constant-temperature bath. The complexes $[PtMe_2(dppm)]$[9] and

Received: July 20, 2013
Published: November 15, 2013

Scheme 1

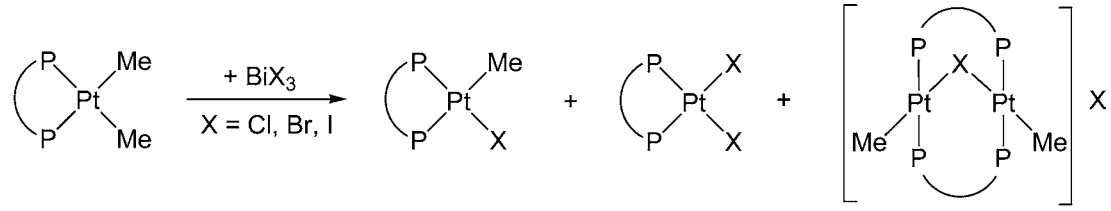

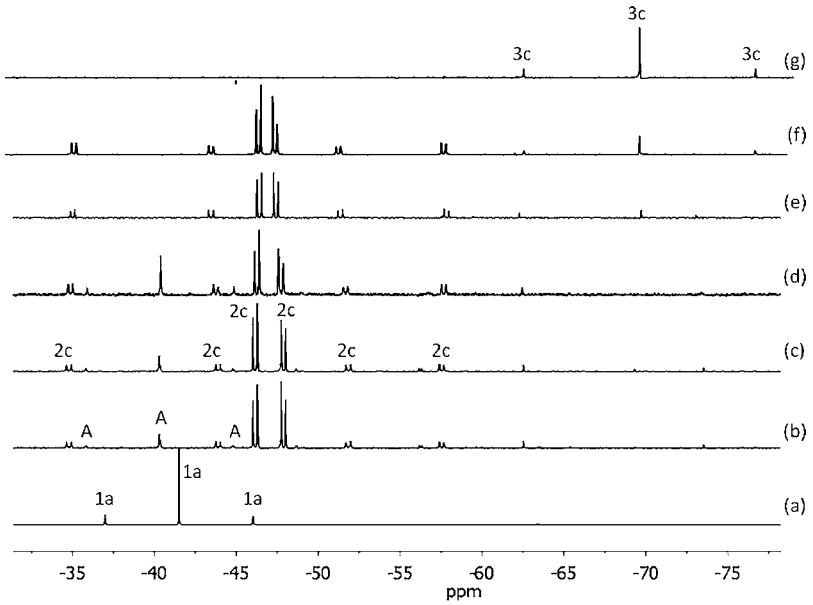

Figure 1. Reaction of complex [$PtMe_2$(dppm)], **1a**, with BiI_3 as monitored by variable-temperature ^{31}P NMR spectroscopy in acetone-d_6; (a) Pure **1a** at −28 °C, (b) immediately after addition of BiI_3 at −28 °C, (c) 6 min after addition of BiI_3 at −28 °C, (d) 12 min after addition of BiI_3 at −8 °C, (e) 18 min after addition of BiI_3 at 16 °C, (f) 25 min after addition of BiI_3 at 27 °C, and (g) 1 h after addition of BiI_3 at 27 °C. Peak assignments are shown; platinum satellites are observed and shown for all involved species.

[$PtMe_2$(dppe)][10] were prepared as reported. The Pt(II) compounds [PtMe(X)(P−P)] (PP = dppm[9] or dppe[11]), **2**, [$Pt(X)_2$(P−P)],[12] **3**, and [$Pt_2Me_2(\mu$-X)(μ-dppm)$_2$]X, **4**,[9b,13] were characterized by comparing their ^1H and ^{31}P NMR spectra with those of the authentic samples. The byproducts of the reactions were $BiMeX_2$ and $BiMe_2X$ which were identified from their reported ^1H NMR data.[14]

Reaction of [$PtMe_2$(dppm)] with $BiCl_3$. To a solution of [$PtMe_2$(dppm)] (50 mg, 0.08 mmol) in 20 mL of acetone was added $BiCl_3$ (25.9 mg, 0.08 mmol). The solution was stirred for 2 h. The solvent was removed, and the resulting residue was dried to form a white solid as a mixture of **3a** and **4a** (see Scheme 1). Selected NMR data for **3a** (30%, minor product) in $CDCl_3$: $\delta(^{31}P)$ −64.0 [s, $^1J_{PtP}$ = 3070 Hz]; $\delta(^1H)$ 4.62 [br, 2H, CH_2P_2]. Selected NMR data for **4a** (70%, major product): $\delta(^{31}P)$ 13.6 [s, $^1J_{PtP}$ = 3033 Hz]; $\delta(^1H)$ 0.50 [t, $^3J_{PH}$ = 8.1 Hz, $^2J_{PtH}$ = 88.0 Hz, 6H, Pt−Me], 4.15 [br, 2H, CH_2P_2].

The following reactions were done similarly by using the appropriate starting complexes **1a** or **1b** and BiX_3 (X = Cl, Br, I).

Reaction of [$PtMe_2$(dppm)] with $BiBr_3$. Selected NMR data for **3b** (50%) in $CDCl_3$: $\delta(^{31}P)$ −63.8 [s, $^1J_{PtP}$ = 3030 Hz]; $\delta(^1H)$ 4.58 [br, 2H, CH_2P_2]. Selected NMR data for **4b** (50%): $\delta(^{31}P)$ 13.5 [s, $^1J_{PtP}$ = 3024 Hz]; $\delta(^1H)$ 0.52 [t, $^3J_{PH}$ = 7.0 Hz, $^2J_{PtH}$ = 85.0 Hz, 6H, Pt−Me], 4.21 [br, 2H, CH_2P_2].

Reaction of [$PtMe_2$(dppm)] with BiI_3. Selected NMR data for **3c** in $CDCl_3$: $\delta(^{31}P)$ −71.1 [s, $^1J_{PtP}$ = 2880 Hz]; $\delta(^1H)$ 4.60 [t, $^2J_{PH}$ = 22.0 Hz, $^3J_{PtH}$ = 34.1 Hz; 2H, CH_2P_2].

Reaction of [$PtMe_2$(dppe)] with $BiCl_3$. Selected NMR data for **2d** in $CDCl_3$: $\delta(^{31}P)$ 44.0 [s, $^1J_{PtP}$ = 1725 Hz, P trans to Me], 43.1 [s, $^1J_{PtP}$ = 4264 Hz, P trans to Cl]; $\delta(^1H)$ 0.62 [dd, $^3J_{P(trans)H}$ = 8.1 Hz, $^3J_{P(cis)H}$ = 3.9 Hz, $^2J_{PtH}$ = 54.0 Hz, 3H, Pt−Me], 2.41 [br, 4H, PCH_2CH_2P].

Reaction of [$PtMe_2$(dppe)] with $BiBr_3$. Selected NMR data in $CDCl_3$, **2e** (70%): $\delta(^{31}P)$ 41.2 [s, $^1J_{PtP}$ = 1745 Hz, P trans to Me], 36.2 [s, $^1J_{PtP}$ = 4241 Hz, P trans to Br]; $\delta(^1H)$ 0.75 [dd, $^3J_{P(trans)H}$ = 8.2 Hz, $^3J_{P(cis)H}$ = 4.1 Hz, $^2J_{PtH}$ = 55.9 Hz, 3H, Pt−Me], 2.33 [br, 4H, PCH_2CH_2P]; **3e** (30%): 44.8 [s, $^1J_{PtP}$ = 3560 Hz].

Reaction of [$PtMe_2$(dppe)] with BiI_3. Selected NMR data in $CDCl_3$, **2f** (50%): $\delta(^{31}P)$ 45.2 [s, $^1J_{PtP}$ = 1725 Hz, P trans to Me], 45.9 [s, $^1J_{PtP}$ = 4072 Hz, P trans to I]; $\delta(^1H)$ 0.80 [dd, $^3J_{P(trans)H}$ = 7.0 Hz, $^3J_{P(cis)H}$ = 3.1 Hz, $^2J_{PtH}$ = 54.1 Hz, 3H, Pt−Me], 2.25 [br, 4H, PCH_2CH_2P]; **3f** (50%): 46.0 [s, $^1J_{PtP}$ = 3375 Hz].

Monitoring the Reaction of [$PtMe_2$(dppm)] with BiI_3 by ^{31}P NMR Spectroscopy. To a solution of [$PtMe_2$(dppm)] (10 mg, 0.016 mmol) in acetone-d_6 (0.7 mL) in an NMR tube was added BiI_3 (9.7 mg, 0.016 mmol). The tube was then placed in the probe of the NMR

dx.doi.org/10.1021/ic4018745 | Inorg. Chem. 2013, 52, 13480−13489

Scheme 2. Suggested Mechanism for the Reactions of Complexes 1 with BiX_3

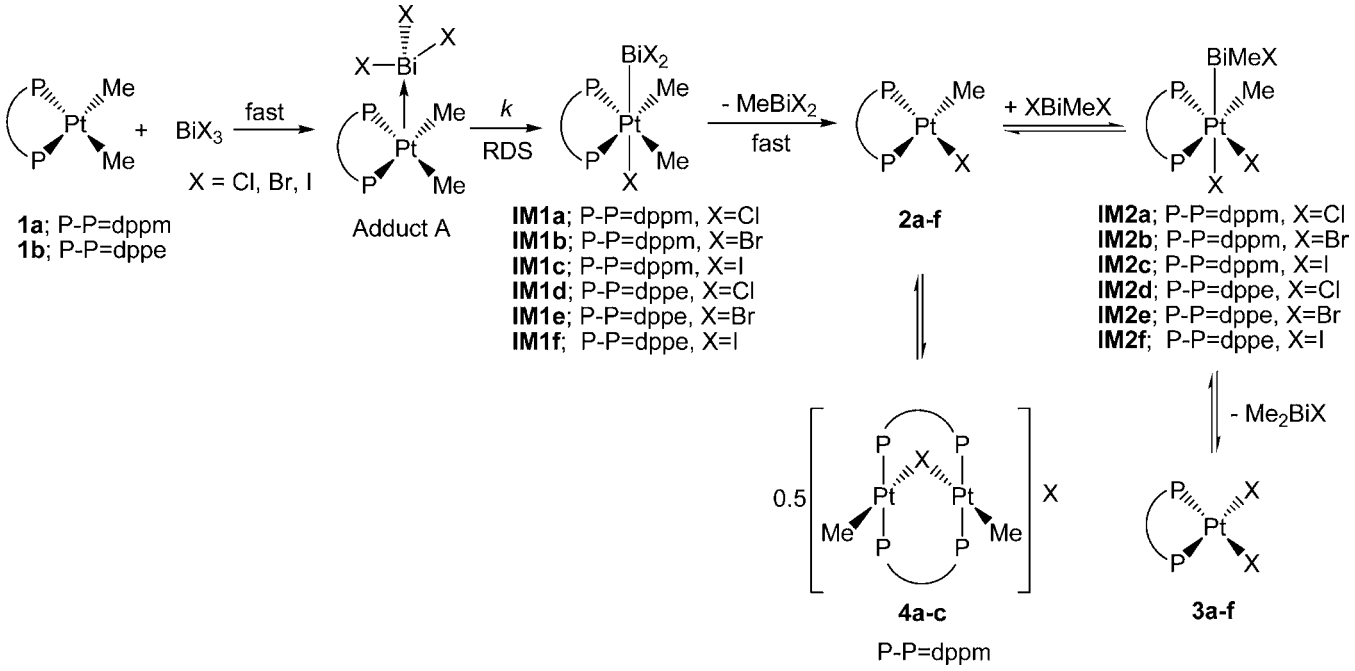

spectrometer, and ^{31}P NMR spectra were obtained at appropriate intervals.

Theoretical Methods. Geometry optimizations were performed with the program suite Gaussian03 at the DFT/B3LYP level.[15] The effective core potential of Hay and Wadt with a double-ξ valence basis set (LANL2DZ)[16] was chosen to describe Pt, Bi, Cl, Br, and I. The 6-31G* basis set was used for C, H, and P atoms. To evaluate and ensure the optimized structures of the molecules, frequency calculations were carried out using analytical second derivatives. The bond orders were calculated using the Chemissian program.[17]

RESULTS AND DISCUSSION

Reactions of Dimethylplatinum(II) Complexes with BiX_3. As is depicted in Scheme 1, reaction of the complexes $[PtMe_2(P-P)]$, **1**, with BiX_3 in 1:1 molar ratio gave a mixture of the monomeric complexes $[PtMe(X)(P-P)]$, **2**, and $[Pt(X)_2(P-P)]$, **3**, and the binuclear complex $[Pt_2Me_2(\mu\text{-}X)(\mu\text{-dppm})_2]X$, **4**. The products were characterized using ^{31}P and ^{1}H NMR spectroscopy, details of which are described in the Experimental Section.

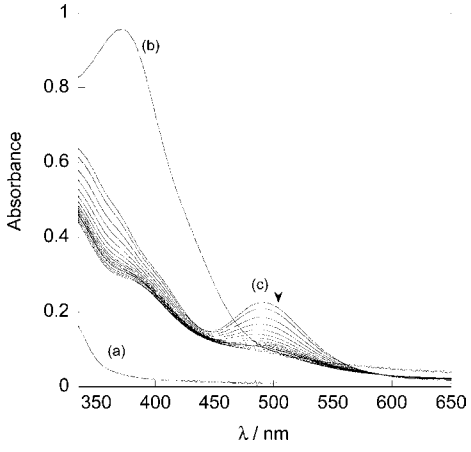

Figure 2. Changes in the UV–vis spectrum during the reaction of $[PtMe_2(dppm)]$ with BiI_3 (each 1.0×10^{-4} M) in acetone at 25 °C: (a) pure **1a**; (b) pure BiI_3; (c) spectrum immediately after addition of BiI_3; successive spectra recorded at intervals of 30 s.

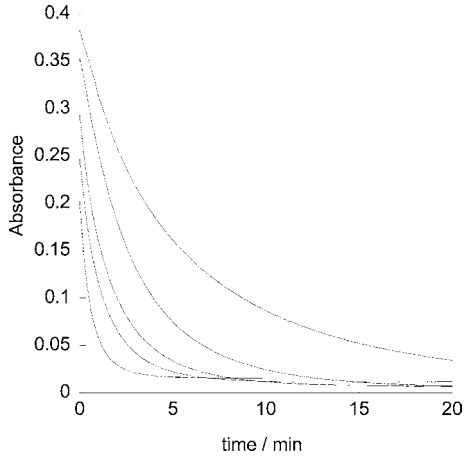

Figure 3. Absorbance (at 490 nm)–time curves for the reaction of $[PtMe_2(dppm)]$, **1a**, with BiI_3 in acetone at temperatures of 10, 20, 25, 30, and 40 °C (temperature increases reading downward).

The reaction of chelating dppm complex **1a** with BiI_3 was monitored using variable-temperature ^{31}P NMR spectroscopy, as shown in Figure 1. On the basis of the results obtained from the ^{31}P NMR and UV–vis spectroscopies (see next section), a mechanism described in Scheme 2 is suggested to occur during the reaction progress. Note that complexes **1a**, **2c**, and **3c** were characterized by comparing their ^{1}H and ^{31}P NMR spectra with those of the authentic samples and so their characteristic ^{31}P NMR data were used to indicate the complexes. Thus, immediately after the addition of BiI_3 at −28 °C, a broad singlet signal at δ −40.3 (with $^{1}J_{PtP}$ = 1455 Hz) which is assigned to a Pt(II)→Bi(III) adduct $BiI_3{\cdot}[PtMe_2(dppm)]$, **A** (see Scheme 2), was observed.[18] The formation of adduct **A** was further confirmed using UV–vis studies (see next section). Meanwhile, a Pt(II) species assigned as the complex [PtMeI-

dx.doi.org/10.1021/ic4018745 | Inorg. Chem. 2013, 52, 13480–13489

Table 1. Rate Constants[a] and Activation Parameters for Oxidative Addition of Bi−X Bonds to Complex 1a in Acetone Solvent

reagent	T/°C	10^2 k/s^{-1}	$\Delta H^{\ddagger}$/kJ mol^{-1}	$\Delta S^{\ddagger}$/J K^{-1} mol^{-1}
$BiCl_3$	10	0.90	52.8 ± 4.3	−98 ± 14
	20	1.52		
	25	2.86		
	30	4.12		
	40	7.89		
$BiBr_3$	10	0.51	55.7 ± 2.9	−99 ± 10
	20	1.00		
	25	1.53		
	30	2.56		
	40	5.19		
BiI_3	10	0.17	51.9 ± 3.9	−115 ± 13
	20	0.30		
	25	0.43		
	30	0.75		
	40	1.45		

[a]Estimated errors in k values are ±5%.

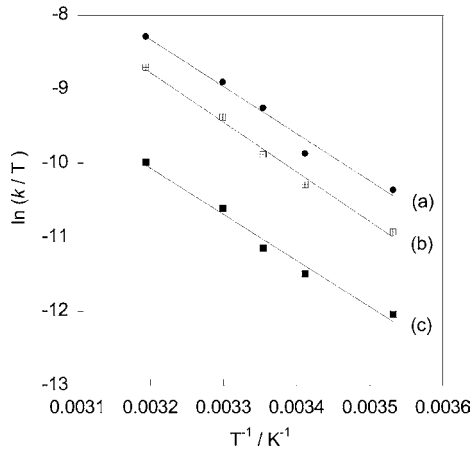

Figure 4. Eyring plots for the oxidative addition of complex **1a** with (a) $BiCl_3$; (b) $BiBr_3$; (c) BiI_3 in acetone.

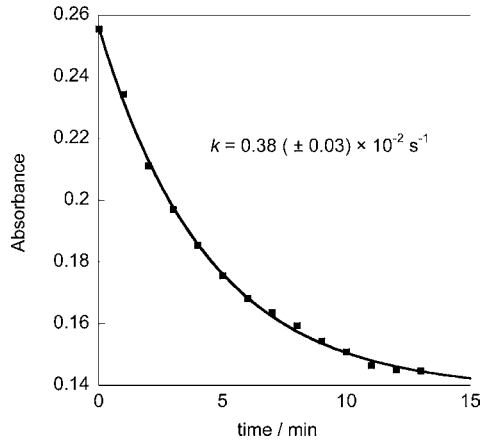

Figure 5. Absorbance−time curve for the reaction of $[PtMe_2(dppe)]$, **1b**, with $BiBr_3$, under 1:1 stoichiometric condition, in acetone at 25 °C. The monoexponential fit for the reaction is shown.

(dppm)], **2c**, was also detected with two doublet signals at δ −46.5 (with $^1J_{PtP}$ = 3702 Hz and $^2J_{PP}$ = 45 Hz, due to P atom trans to I) and at δ −47.3 (having a significantly lower value of $^1J_{PtP}$ = 1279 Hz, due to the P atom locating trans to Me with comparatively higher trans influence than I,[19] and $^2J_{PP}$ = 45 Hz). As time passed and the temperature increased, the signal due to adduct **A** disappeared while those due to the complex **2c** grew and then later started to decrease, and meanwhile a comparatively weak singlet signal, at δ −69.8 with $^1J_{PtP}$ = 2866 Hz, due to the monomeric complex $[PtI_2(dppm)]$, **3c**, was also observed. As the reaction progressed, only complex **3c** obtained pure which was found by DFT to be more stable as compared to complex **2c** (see theory section). The ^{1}H NMR spectrum was recorded at the end of the reaction, and the observation of one singlet signal at δ 2.27 ppm confirmed the formation of $BiMe_2I$.

UV−visible Studies of the Reaction of $[PtMe_2(dppm)]$, 1a, with BiX_3. The kinetics of the reaction of equimolar amounts of complex $[PtMe_2(dppm)]$, **1a**, and bismuth trihalides in acetone solution were studied by using UV−vis spectroscopy. A series of spectra, recorded during the reaction of complex **1a** with BiI_3, is shown in Figure 2. The complex **1a** is colorless, and no MLCT band in the visible region was observed for this complex. Immediately after addition of BiI_3 to a solution of complex **1a** under second-order 1:1 stoichiometric conditions, a new broad absorption band at 490 nm was observed. It is worthy to mention that when we performed the reaction in the presence of excess BiI_3, the reaction was too fast for any reasonable measurement. The absorption at 490 nm is ascribed to the $5d_\pi$ (Pt)→(Bi−I σ^*-orbital) charge transfer band, which is suggested to be responsible for the yellowish color of the adduct **A** and is used to study the kinetics of the oxidative addition reaction. The assignment of this absorption to other complexes, shown in Scheme 2, is ruled out because the intermediates **IM1** and **IM2** containing Pt(IV) center are not expected to contain any charge transfer and complexes **1**, **2**, **3**, and **4** are colorless. Notice that it has been reported that the complex $[PtCl(PCy_3)_2\{BiCl_2\}]$, having a Pt(II)−Bi(III) bond, has an orange color in tetrahydrofuran (THF) solution.[4] Also formation of such adducts for Pt(II) complexes has been reported in the reaction of $[PtMe_2(bipy)]$ with iodine.[8e] On the basis of a fully optimized ground-state structure (see theory section), time-dependent TDF (TD-DFT) has been also used to predict the absorbance spectra of adduct **A** and intermediate **IM1c**. For adduct **A**, the TD-DFT calculation predicts one intense electronic transition at 477 nm in good agreement with the observed experimental data ($\lambda_{exp.}$ = 490 nm in acetone). The calculated electronic spectrum of complex **IM1c** shows one electronic transition at 384 nm. As is clear from TD-DFT calculation, the observed experimental wavelength at 490 nm is in good agreement with the calculated one for adduct **A**, giving more support for the assignment of yellowish color to adduct **A**.

From the ^{31}P NMR and UV−vis observations, the formation of the adduct **A** was too fast for monitoring, but the conversion of the adduct **A** to form Pt(IV) intermediate **IM1c** could be studied by monitoring the decay of the absorption band of the adduct **A** at 490 nm. Typical plots of absorbance at λ = 490 nm versus time are shown in Figure 3. The disappearance of the adduct **A** to form the intermediate complex **IM1c** followed good first-order kinetics, as confirmed by fitting the data with the first order equation $A_t = (A_0 - A_\infty)\exp(-kt) + A_\infty$. The first order rate constants at different temperatures are given in Table 1. Activation parameters were then obtained in the usual way from the Eyring equation (Figure 4), and the data are collected in Table 1.

dx.doi.org/10.1021/ic4018745 | Inorg. Chem. 2013, 52, 13480−13489

Scheme 3. Structural Changes in Oxidative Addition of $BiCl_3$ to Complex $[PtMe_2(dppm)]$, 1a, and the Optimized Geometries in Acetone Solvent

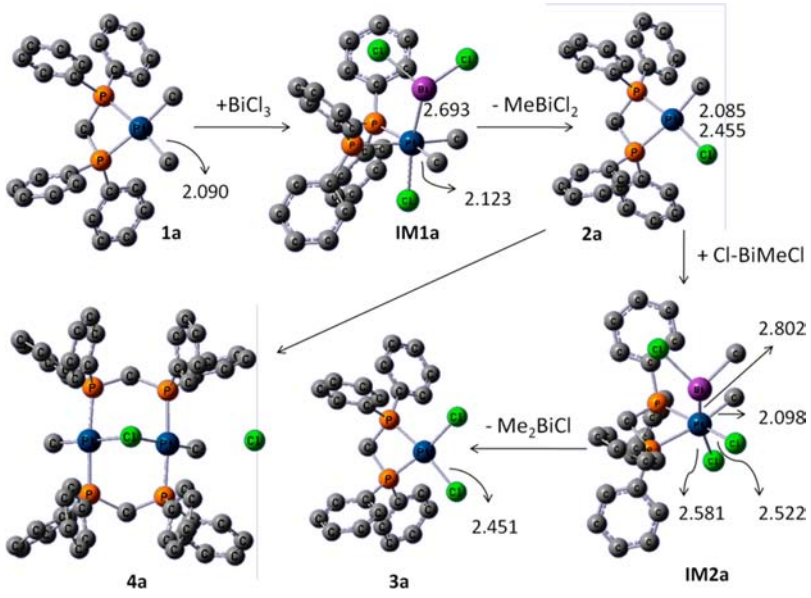

Table 2. Computed Reaction Enthalpies and Free Energies (Values in kcal mol^{-1}) for Each Step Reaction of BiX_3 (X = Cl, Br, I) with $[PtMe_2(P{-}P)]$, P−P =dppm, 1a; P−P =dppe,1b, in Acetone

	X = Cl		X = Br		X = I	
reaction	ΔH	ΔG^a	ΔH	ΔG^a	ΔH	ΔG^a
			P−P = dppm			
1a + BiX_3→**IM1**	−22.5	−8.4	−20.9	−6.4	−17.9	−1.8
IM1→**2** + $MeBiX_2$	−12.4	−26.7	−15.3	−29.6	−17.6	−32.8
2 → (1/2) **4**	2.6	7.3	0.9	5.7	0.7	5.8
2 + XBiMeX→**IM2**	10.9	24.8	12.2	26.3	13.3	28.1
IM2→**3** + Me_2BiX	−18.9	−32.0	−20.2	−34.0	−22.0	−36.4
			P−P = dppe			
1b + BiX_3→**IM1**	−17.8	−5.4	−15.7	−3.4	−12.2	1.1
IM1→**2** + $MeBiX_2$	−16.2	−30.4	−19.2	−33.7	−22.2	−37.3
2 + XBiMeX→**IM2**	6.0	28.1	19.0	36.9	21.8	38.3
IM2→**3** + Me_2BiX	−24.3	−36.4	−27.1	−45.3	−29.7	−45.5

[a]At 298.15 K and 1 atm.

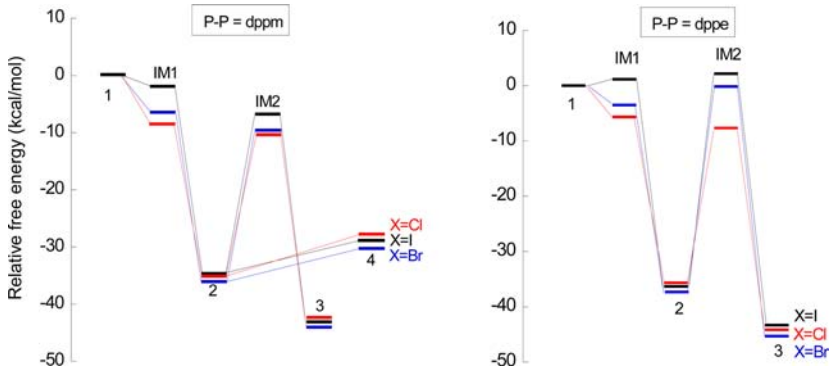

Figure 6. Free energy profiles for reaction of BiX_3 (X = Cl, Br, I) with $[PtMe_2(dppm)]$ (left) and $[PtMe_2(dppe)]$ (right) in acetone.

When the reaction of complex $[PtMe_2(dppe)]$, **1b**, with $BiBr_3$ was performed in acetone at 25 °C, the oxidative addition process (see Figure 5) occurred at a slower rate, with k = 0.38 (±0.03) × 10^{-2} s^{-1}, as compared with the value of k = 1.53 (±0.07) × 10^{-2} s^{-1} for the related reaction involving dppm complex $[PtMe_2(dppm)]$, **1a**, at the same condition.

DFT Investigation of the Product Formation. The oxidation state +2 (d^8) is undoubtedly the most common oxidation state for Pt metal. The stereochemistry of Pt(II) four coordinate complexes is square planar especially with strong field ligands such as methyl. The oxidative addition process is considered here with an emphasis on the differences between

dx.doi.org/10.1021/ic4018745 | Inorg. Chem. 2013, 52, 13480−13489

Table 3. Energies (eV) and Main Compositions (%) of the Relevant Frontier Orbitals of Species Involved in the Reaction of Complex 1a with $BiCl_3$ (X = Cl, Br, I)

			composition (%)		
	orbital	E (eV)	Pt	Bi	X[a]
$[PtMe_2(dppm)]$	HOMO	−5.137	70		
	LUMO	−1.002	3		
$BiCl_3$	HOMO	−8.720			100
	LUMO	−3.370		60	40
$BiBr_3$	HOMO	−8.117			100
	LUMO	−3.648		56	44
BiI_3	HOMO	−7.534			100
	LUMO	−3.989		56	44
$[PtCl(BiCl_2)Me_2(dppm)]$, **IM1a**	HOMO	−6.056	16	10	52
	LUMO	−1.961	23	41	9
$[PtBr(BiBr_2)Me_2(dppm)]$, **IM1b**	HOMO	−5.789	9	5	70
	LUMO	−2.271	21	43	10
$[PtI(BiI_2)Me_2(dppm)]$, **IM1c**	HOMO	−5.527	6	3	78
	LUMO	−2.591	19	44	10
$[PtMe(Cl)(dppm)]$, **2a**	HOMO	−5.447	25		41
	LUMO	−1.237	3		1
$[PtMe(Br)(dppm)]$, **2b**	HOMO	−5.247	18		58
	LUMO	−1.263	2		1
$[PtMe(I)(dppm)]$, **2c**	HOMO	−4.979	12		71
	LUMO	−1.306	5		1
$[Pt(Cl)_2(BiMeCl)Me(dppm)]$, **IM2a**	HOMO	−5.808	21	15	46
	LUMO	−2.301	27	20	14
$[Pt(Br)_2(BiMeBr)Me(dppm)]$, **IM2b**	HOMO	−5.577	8	1	83
	LUMO	−2.529	26	22	16
$[Pt(I)_2(BiMeI)Me(dppm)]$, **IM2c**	HOMO	−5.319	5	1	86
	LUMO	−2.727	25	22	20
$[Pt(Cl)_2(dppm)]$, **3a**	HOMO	−5.763	26		68
	LUMO	−1.502	26		11
$[Pt(Br)_2(dppm)]$, **3b**	HOMO	−5.513	1		77
	LUMO	−1.696	24		13
$[Pt(I)_2(dppm)]$, **3c**	HOMO	−5.099	2		86
	LUMO	−1.740	25		18

[a]Coordinated to Pt in platinum complexes.

the nature of the halides (Cl, Br, and I) in three bismuth(III) halides. The processes shown in Scheme 2 will be explored on the basis of DFT calculations.

In the related reaction profile in acetone solvent, shown in Scheme 3 (see Table 2 for calculated results), the metal center of $[PtMe_2(P-P)]$ attacks the bismuth atom of the oxidative addition reagent BiX_3 while the X atom leaves and the Pt(IV) complex, **IM1**, is formed. As such, the Pt−Me and Pt−Bi bond distances vary more substantially than any other bond lengths. For example as shown in Scheme 3, in the case of P−P = dppm and X = Cl, the Pt−C(Me) distance increases from 2.090 Å in complex **1a** to 2.123 Å in intermediate **IM1a**, whereas the Pt−Bi distance decreases from far apart in reactant **1a** and $BiCl_3$ to 2.693 Å in intermediate **IM1a**. In the intermediate **IM1**, one of the Bi−X bonds is completely broken while the Pt−Bi bond is formed. The resulting d^6 complex $[PtX(BiX_2)Me_2(P-P)]$ (X = Cl, Br, I) adopts an octahedral conformation with the bismuth group BiX_2 and X being in the trans position. The Pt(IV) complexes $[PtX(BiX_2)Me_2(dppm)]$, **IM1**, easily undergo X_2Bi-Me reductive elimination to produce complexes **2**. Then the Pt(II) center of complex **2** attacks to the bismuth atom of X−BiXMe under a second oxidative addition process to form the Pt(IV) intermediates **IM2**. The complex **IM2** contains two Pt−X bonds, one trans to a P atom and another trans to a BiMeX group with different bond lengths. For example, in complex **IM2a**, these Pt−Cl bond distances are 2.522 and 2.581 Å, respectively. During the oxidative addition of Cl−BiClMe bond to complex **2a**, the Pt−Me, Pt−P (trans to Me), Pt−P (trans to Cl), and Pt−Cl bond distances increase from 2.085, 2.430, 2.257, and 2.455 Å in complex **2a** to 2.098, 2.540, 2.318, and 2.522 Å in complex **IM2a**, respectively (see Scheme 3). The Pt−Bi distance decreases from far apart in reactant **2a** and Cl−BiClMe to 2.802 Å in intermediate **IM2a**. Finally, the Me−BiMeX reductive elimination from **IM2** occurs easily to form more stable complex **3**.

Free energy changes along these paths are given in Figure 6. We found that the first oxidative addition of BiX_3 to the Pt(II) complexes **1** to yield the complexes **IM1** is exergonic for most of halides and span a range of 1.1 kcal mol^{-1} to −8.4 kcal mol^{-1} as shown in Table 2 and Figure 6. When P−P = dppm, the free energies of this process (**1** + BiX_3→**IM1**) are slightly lower than the related free energies calculated for P−P = dppe which is due to presence of ring strain in 4-membered rings of dppm complexes. The second oxidative addition reactions (i.e., **2** + XBiMeX →**IM2**) are endergonic for all halides and P−P. This suggests that the second oxidative addition is more difficult compared to the first oxidative addition, probably because of the presence of a halide ligand which reduces the electron

dx.doi.org/10.1021/ic4018745 | Inorg. Chem. 2013, 52, 13480−13489

Scheme 4. Suggested Mechanism for Oxidative Addition of BiI_3 to Complex 1a and Bi−C Reductive Elimination Form Complex IM1c

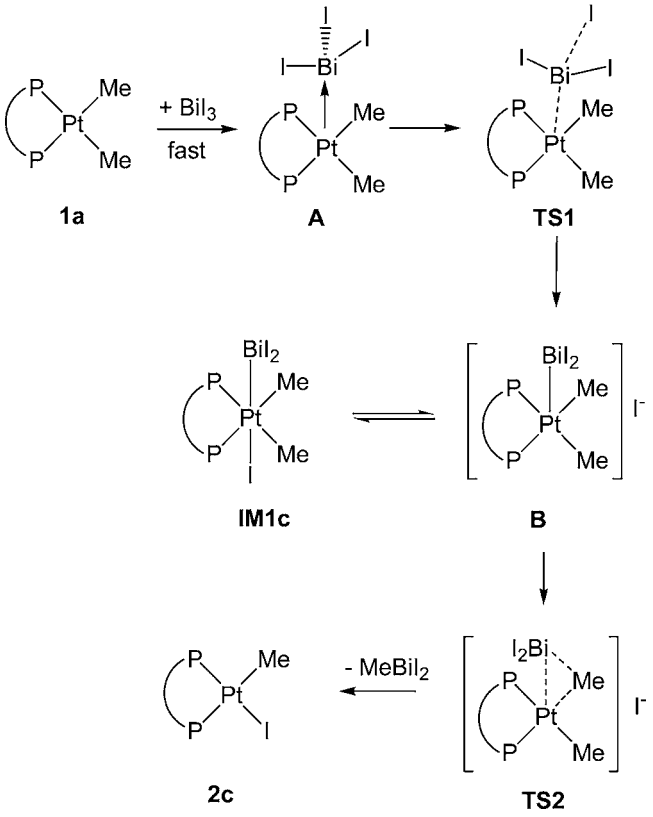

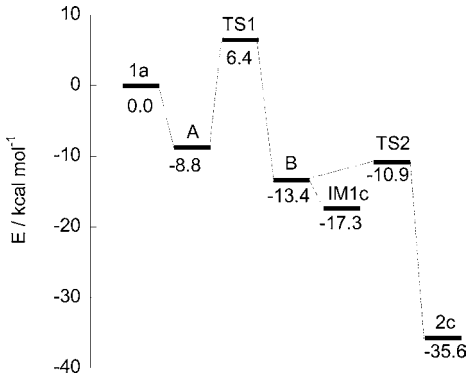

Figure 7. Relative energies (kcal mol^{-1}) for product **2c**, adduct **A**, intermediate **IM1c** and **B**, and transition states **TS1** and **TS2**, arising from the reaction of **1a** + BiI_3 (E = 0) in acetone solution.

density of Pt(II) center in complexes **2**. As shown in Table 3 (see next section), in [$PtMe_2$(dppm)] as an example, the highest occupied molecular orbital (HOMO) is localized on the platinum atom (70% Pt) with significant contribution of the d_{z^2} orbital, but in complex [PtMe(Cl)(dppm)], **2a**, the composition of the HOMO is 25% Pt + 41% X, showing a transmission of electron density from the Pt atom to the X atom.

While the free energy for both steps of oxidative addition (**1** + BiX_3→**IM1** and **2** + XBiMeX→**IM2**) decreases in the order X = Cl > Br > I, both reductive elimination reactions (**IM1**→**2** + $MeBiX_2$ and **IM2**→**3** + Me_2BiX) are exergonic for all halides, and the trend for free energy of these reactions decreases in the order X = Cl < Br < I. For example when P−P = dppm, the free energies for the reaction **1** + BiX_3→**IM1** are −8.4, −6.4, and −1.8 kcal mol^{-1} for X = Cl, Br, and I, respectively. On the basis of HSAB (hard and soft acids and bases) principles, the Pt(IV) center is harder than the Pt(II) center, and the preference for halides toward the Pt(IV) center follows the order Cl > Br > I. Conversely, the free energies for the reductive elimination reactions **IM1**→**2** + $MeBiX_2$ are −26.7, −29.6, and −32.8 kcal mol^{-1} for X = Cl, Br, and I, respectively. This can also be explained on the basis of the HSAB principle, which suggests the preference for the halides as Cl < Br < I for the soft Pt(II) center of complexes **2**.

The HSAB principle can also be used to explain the experimental product ratios in the reactions of BiX_3 with complexes **1**. The percentage of complexes **3**, compared to complexes **2**, increases according to Cl < Br < I. For example in the reaction **1a** with BiX_3, the percentage of complexes **3** is 30, 70, and 100% for X = Cl, Br, and I, respectively. The same was observed in the reaction of **1b** with BiX_3 as 0, 30, and 50% for X = Cl, Br, and I, respectively. The preference of X toward the soft Pt(II) center is I > Br > Cl, so due to the greater tendency of I to bind the soft Pt(II) center, the ratio of complexes **3** with two X ligands will be increased as I > Br > Cl. The free energies for reductive elimination processes have large negative values (ranging from −26.7 to −36.4 kcal mol^{-1} for P−P = dppm and from −5.4 to −45.5 kcal mol^{-1} when P−P = dppe).

While the Pt(IV)−M complexes (M = Sn, Hg, Te, and Ge) can simply be prepared,[3b,d,e,i] the related Pt(IV)−Bi(III) analogues are not stable and easily undergo Bi−C reductive elimination. To verify this, we calculated the reaction profiles and energies for the Bi−I oxidative addition to complex **1a** and Bi−C reductive elimination from the intermediate complex **IM1c** in acetone solution (see Scheme 4 and Figure 7). The calculation indicates an easy reaction to give the adduct **A**, followed by a slower reaction to give **B** and **IM1c**. Note that, in the kinetic experiments, the loss of adduct **A** is measured so that the rates refer to formation of **IM1c**. The calculation of the energy of the transition state **TS1** (+15.2 kcal mol^{-1}) is in reasonable agreement with the observed value of $\Delta H^{\ddagger}$ = 12.4 kcal mol^{-1}. It is suggested that the reductive elimination from 5-coordinate d^6 metal complexes occurs more easily than from the corresponding 6-coordinate complexes.[20] So, the Me-BiI_2 reductive elimination from the saturated d^6 six-coordinate complex **IM1c** may occur via initial loss of iodide ligand. The $BiMeI_2$ reductive elimination from intermediate **B** proceeds through transition state **TS2**, (Scheme 4), in which the bonds between Pt and leaving groups (Me and BiI_2) are elongated and the Me−Pt-Bi bond angle is reduced. The free energy of activation for reductive elimination process is 6.4 kcal mol^{-1}. As $BiMeI_2$ dissociates, the Pt(II)−I bond is formed giving the complex **2c**. Our calculations show that following oxidative addition, the Bi−C reductive elimination barrier is rather small suggesting that the Pt(IV)−Bi(III) complex is very prone to undergo the reductive elimination decreasing the possibility of identifying the Pt(IV) complexes from the experimental point of view which is consistent with the experimental observations. Figure 6 shows free energy profiles for reaction of BiX_3 (X = Cl, Br, I) with [$PtMe_2$(dppm)] (left) and [$PtMe_2$(dppe)] (right) in acetone.

Structural Investigation of Pt(IV)−Bi(III) Intermediates. Since dihalobismuth complexes of platinum(IV) are not known so far, we discuss here the structures of these Pt(IV)−BiX_2 (X = Cl, Br, I) intermediate complexes (**IM1a−f**). Upon going from X = Cl to X = I, the trend for the calculated Pt−Bi

dx.doi.org/10.1021/ic4018745 | Inorg. Chem. 2013, 52, 13480−13489

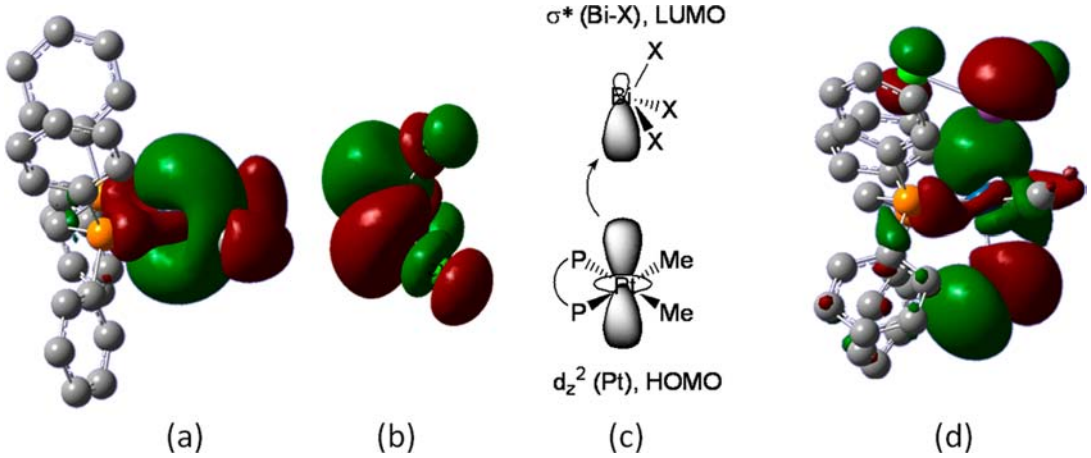

Figure 8. (a) HOMO of [$PtMe_2$(dppm)], (b) LUMO of $BiCl_3$, (c) interactions of Lewis acidic bismuth center of BiX_3 with electron-rich Pt(II) center of [$PtMe_2$(dppm)] and (d) HOMO of [$PtCl(BiCl_2)Me_2$(dppm)], **IM1a**.

bond distance in the complexes [$PtX(BiX_2)Me_2$(dppm)] increases as 2.693 Å (**IM1a**) < 2.719 Å (**IM1b**) < 2.752 Å (**IM1c**). The well−known trans influence of the halides (bound to M) follows the order $I^- > Br^- > Cl^-$; that is, the strength of the Pt−Bi bond decreases on going from X = Cl to X = I in the complexes [$PtX(BiX_2)Me_2$(dppm)]. This is in agreement with the bond orders calculated for Pt−Bi bonds in complexes **2** (0.712, 0.677, and 0.638 for X = Cl, Br, and I, respectively). The same behaviors have been observed for complexes [$Pt(X)_2$(BiMeX)Me(dppm)], **IM2a−c**, and dppe complexes (**IM1d−f** and **IM2d−f**). The Pt−X optimized bond distances, 2.565, 2.721, and 2.916 Å, for X = Cl, Br, and I in **IM1a**, **IM1b**, and **IM1c**, respectively, are longer than that expected for the single Pt−X bond on the basis of covalent radii predictions (Pt−Cl = 2.28 Å, Pt−Br = 2.43 Å, Pt−I = 2.62 Å). The calculated bond orders of the optimized Pt−X bond distances in these complexes are 0.83 (X = Cl; **IM1a**), 0.79 (X = Br; **IM1b**), and 0.76 (X = I; **IM1c**). The optimized Bi−X bond distances, 2.525, 2.764, and 2.915 Å in complexes **IM1a**, **IM1b**, and **IM1c**, respectively, are slightly longer than that expected for the single Bi−X bond on the basis of covalent radii predictions (Bi−Cl = 2.51 Å, Bi−Br = 2.66 Å, Bi−I = 2.85 Å). The X−Pt−Bi bond angles in these complexes are almost linear. The geometry at bismuth is that of a distorted trigonal pyramid with the X−Bi−X and Pt−Bi−X bond angles in the range 95−106°.

Frontier Molecular Orbitals. Qualitative representations of the HOMO of [$PtMe_2$(dppm)] and lowest unoccupied molecular orbital (LUMO) of $BiCl_3$ are presented in Figure 8, and their composition and energy of the starting materials, intermediates, and products are reported in Table 3. The HOMO−LUMO gap of [$PtMe_2$(dppm)] is equal to 4.135 eV. In [$PtMe_2$(dppm)], platinum is formally d^8 and as expected the HOMO is localized on the platinum atom with significant contribution of the d_{z^2} orbital. The value of the energy separations between the HOMO and LUMO of [$PtX(BiX_2)$-Me_2(dppm)], **IM1**, are equal to 4.095 (X = Cl), 3.518 (X = Br), and 2.936 (X = I) eV. The main contribution to the Pt−Bi in the Pt(IV) complexes, **IM1**, comes from the overlap of the d_{z^2} HOMO of the platinum complex with the LUMO of BiX_2 (which is σ^* orbital of Bi−X bond). So it is reasonable to view the oxidation process formally as the removal of electrons from the HOMO of the [$PtMe_2$(dppm)] complex into the LUMO of BiX_3.

CONCLUSION

The reaction of organoplatinum(II) complexes [$PtMe_2$(P−P)], P−P = dppm or dppe, with bismuth trihalides proceeds through bismuth−halide oxidative addition and bismuth−carbon reductive elimination reactions to yield a mixture of the platinum(II) complexes [PtMeX(P−P)], **2**, and [Pt-$(X)_2$(P−P)], **3** (X = Cl, Br, I). These reactions, which are the first examples of addition of bismuth trihalides to organoplatinum(II) complexes, were monitored using ^{31}P NMR and UV−vis spectroscopy, and a mechanism shown in Scheme 2 is proposed for the reaction. As such, immediately after the addition of BiX_3 to the starting complex [$PtMe_2$(P−P)], **1**, the platinum(II) center, which is electron rich, orients its filled d_{z^2} orbital to the empty σ^* (Bi−X) orbital of BiX_3 to form a yellowish Pt(II)→Bi(III) adduct, **A**, with λ = 490 nm in acetone solvent. The rate of this step is too fast to measure, but the rate of conversion of the yellowish adduct **A** to the colorless Pt(IV)−Bi(III) intermediate **IM1** was easily monitored by the decay of the absorption band of the Pt(II)→Bi(III) adduct (see Figure 2). Note that the addition occurs by loss of X from **A**, followed by attack by X opposite the BiX_2 group. The nature of halide has an effect on the rates of oxidative addition of BiX_3 to Pt(II) complexes; the process becomes slower as the halide becomes larger (see Table 1). This complies with the suggested mechanism in a way that when the d_{z^2} orbital of Pt(II) center donates its electron density into the empty σ^*(Bi−Cl) orbital of $BiCl_3$, which is a stronger Lewis acid as compared with $BiBr_3$ and BiI_3, the Bi−Cl becomes weaker, as compared to Bi−Br and Bi−I, which makes transfer of Cl^- to the Pt center, to form

Scheme 5

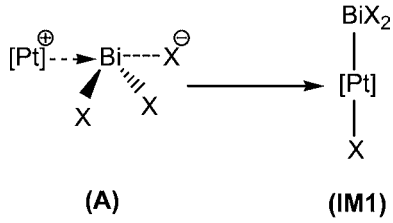

[Pt] = [$PtMe_2$P-P]

dx.doi.org/10.1021/ic4018745 | Inorg. Chem. 2013, 52, 13480−13489

Table 4. Enthalpy Changes for Reductive Elimination of Some C−Y Bonds from Pt(IV) Complexes

reaction	C−Y	ΔH/kcal mol^{-1}	ref.
$[PtMe_3I(dppe)] \rightarrow [PtMe_2(dppe)] + MeI$	C−I	14.4	6a
$[PtMe_3I(dppe)] \rightarrow [PtMeI(dppe)] + C_2H_6$	C−C	−25.1	6a
$[PtI(BiI_2)Me_2(dppm)] \rightarrow [PtIMe(dppm)] + BiI_2Me$	C−Bi	−17.6	this work
$[PtI(BiI_2)Me_2(dppe)] \rightarrow [PtIMe(dppe)] + BiI_2Me$	C−Bi	−22.2	this work

IM1, easier with a greater rate (see Scheme 5). The same line of reasoning goes with the other two halides $BiBr_3$ and BiI_3.

Consistent with this mechanism, the rate of conversion involving the starting dppm complex $[PtMe_2(dppm)]$, **1a**, in reaction with $BiBr_3$ [k = 1.53 (±0.07) × 10^{-2} s^{-1}] at 25 °C is nearly 3 times greater than that involving the starting dppe complex $[PtMe_2(dppe)]$, **1b**, at the same condition [k = 0.38 (±0.03) × 10^{-2} s^{-1}]. Here, according to DFT calculations, the Pt center of adduct **A** containing dppm is less positive and more electron rich, as compared to that containing dppe. This makes the Pt−Bi bond weaker in adduct **A** with a dppm ligand (with the greater rate of conversion) than that involving a dppe ligand (with the smaller rate of conversion).

A theoretical study is presented where the structure of all intermediates containing neutral bismuth complexes of platinum are investigated. It is shown that the oxidative addition of BiX_3 to the Pt(II) complex is exergonic for all bismuth halides. The operative mechanism is suggested to involve nucleophilic attack of platinum(II) center (occupied d_{z^2} orbital) on the bismuth atom of BiX_3 (σ^* orbital of Bi−X bond) to give the platinum(IV) intermediates, $[PtX(BiX_2)Me_2(P-P)]$, which undergo reductive elimination. The free energies for oxidative addition steps involved in the reactions decrease in the order X = Cl > Br > I and dppe > dppm, while it increases for the reductive elimination step as I < Br < Cl. The reductive elimination of X_2Bi-CH_3 from the Pt(IV)−Bi(III) complex is thermodynamically favored by heavier halides, largely because of a change in enthalpy. The enthalpy changes for reductive elimination of some C−Y (Y = C, Bi, and I) bonds from Pt(IV) complexes are shown in Table 4. The reductive elimination of C−C and C−Bi bonds are clearly favored over C−I, and enthalpy values decrease as C−I > C−Bi > C−C. DFT calculations show that the Pt(IV)−Bi(III) complexes are not stable and immediately would undergo Bi−C reductive elimination. Note that no Pt(IV)−Bi(III) octahedral complex has been reported so far.

AUTHOR INFORMATION

Corresponding Authors

*E-mail: nabavi@chem.susc.ac.ir (S.M.N.).

*E-mail: niroomand@iaushiraz.ac.ir (F.N.H.).

Notes

The authors declare no competing financial interest.

ACKNOWLEDGMENTS

We thank the Iran National Science Foundation (Grant No. 90004861), the Shiraz University Research Council, and the Islamic Azad University, Shiraz Branch, for financial support. We gratefully acknowledge Professor Mehdi Rashidi's scientific influence on our investigations, and his valuable discussion and encouragement. We wish to thank SUSC Computer Center for providing computer facilities, Dr. N. Mogharab and M. Abdolahi for assisting us in our use of these facilities and for help with our day-to-day computer related tasks at SUSC computer Center.

REFERENCES

(1) (a) Chauhan, R. S.; Prabhu, C. P.; Phadnis, P. P.; Kedarnath, G.; Golen, J. A.; Rheingold, A. L.; Jain, V. K. *J. Organomet. Chem.* **2013**, *723*, 163. (b) Safa, M.; Puddephatt, R. J. *J. Organomet. Chem.* **2013**, *724*, 7. (c) Momeni, B. Z.; Rashidi, M.; Jafari, M. M.; Patrick, B. O.; Abd-El-Aziz, A. S. *J. Organomet. Chem.* **2012**, *700*, 83. (d) Bette, M.; Rüffer, T.; Bruhn, C.; Schmidt, J.; Steinborn, D. *Organometallics* **2012**, *31*, 3700. (e) Calvet, T.; Crespo, M.; Font-Bardía, M.; Jansat, S.; Martínez, M. *Organometallics* **2012**, *31*, 4367. (f) Mazzone, G.; Russo, N.; Sicilia, E. *Inorg. Chem.* **2011**, *50*, 10091. (g) Margiotta, N.; Ranaldo, R.; Intini, F. P.; Natile, G. *Dalton Trans.* **2011**, *40*, 12877. (h) La Deda, M.; Crispini, A.; Aiello, I.; Ghedini, M.; Amati, M.; Belviso, S.; Lelj, F. *Dalton Trans.* **2011**, *40*, 5259. (i) Clot, E.; Eisenstein, O.; Jasim, N.; Macgregor, S. A.; McGrady, J. E.; Perutz, R. N. *Acc. Chem. Res.* **2011**, *44*, 333. (j) Hamilton, M. J.; Puddephatt, R. J. *Inorg. Chim. Acta* **2011**, *369*, 190. (k) Bonnington, K. J.; Jennings, M. C.; Puddephatt, R. J. *Organometallics* **2008**, *27*, 6521.

(2) (a) Kim, S.; Boyle, P. D.; McCready, M. S.; Pellarin, K. R.; Puddephatt, R. J. *Chem. Commun.* **2013**, *49*, 6421. (b) Mitzenheim, C.; Braun, T. *Angew. Chem., Int. Ed.* **2013**, *52*, 8625. (c) Braunschweig, H.; Damme, A. *Chem. Commun.* **2013**, *49*, 5216. (d) Maidich, L.; Zucca, A.; Clarkson, G. J.; Rourke, J. P. *Organometallics* **2013**, *32*, 3371. (e) Rendina, L. M.; Puddephatt, R. J. *Chem. Rev.* **1997**, *97*, 1735.

(3) (a) Momeni, B. Z.; Moradi, Z.; Rashidi, M.; Rominger, F. *Polyhedron* **2009**, *28*, 381. (b) Levy, C. J.; Puddephatt, R. J.; Vittal, J. J. *Organometallics* **1994**, *13*, 1559. (c) Janzen, M. C.; Jenkins, H. A.; Rendina, L. M.; Vittal, J. J.; Puddephatt, R. J. *Inorg. Chem.* **1999**, *38*, 2123. (d) Janzen, M. C.; Jennings, M. C.; Puddephatt, R. J. *Organometallics* **2001**, *20*, 4100. (e) Levy, C. J.; Puddephatt, R. J. *J. Am. Chem. Soc.* **1997**, *119*, 10127. (f) Van der Ploeg, A. F. M. J.; Van Koten, G.; Vrieze, K.; Spek, A. L. *Inorg. Chem.* **1982**, *21*, 2014. (g) Janzen, M. C.; Jennings, M. C.; Puddephatt, R. J. *Inorg. Chem.* **2001**, *40*, 1728. (h) Levy, C. J.; Vittal, J. J.; Puddephatt, R. J. *Organometallics* **1996**, *15*, 2108. (i) Janzen, M. C.; Jennings, M. C.; Puddephatt, R. J. *Inorg. Chem.* **2003**, *42*, 4553.

(4) Braunschweig, H.; Brenner, P.; Cogswell, P.; Kraft, K.; Schwab, K. *Chem. Commun.* **2010**, *46*, 7894.

(5) (a) Sanderson, J.; Bayse, C. A. *Tetrahedron* **2008**, *64*, 7685. (b) Lange, K. C. H.; Klaptoke, T. M. *The Chemistry of Organic Arsenic, Antimony and Bismuth Compounds*; J. Wiley: New York, 1994. (c) Pyykko, P. *Chem. Rev.* **1988**, *88*, 563.

(6) (a) Goldberg, K. I.; Yan, J. Y.; Breitung, E. M. *J. Am. Chem. Soc.* **1995**, *117*, 6889. (b) Williams, B. S.; Goldberg, K. I. *J. Am. Chem. Soc.* **2001**, *123*, 2576. (c) Jensen, M. P.; Wick, D. D.; Reinartz, S.; White, P. S.; Templeton, J. L.; Goldberg, K. I. *J. Am. Chem. Soc.* **2003**, *125*, 8614. (d) Pawlikowski, A. V.; Getty, A. D.; Goldberg, K. I. *J. Am. Chem. Soc.* **2007**, *129*, 10382. (e) Yahav-Levi, A.; Goldberg, I.; Vigalok, A. *J. Am. Chem. Soc.* **2006**, *128*, 8710. (f) Reinartz, S.; White, P. S.; Brookhart, M.; Templeton, J. L. *Organometallics* **2000**, *19*, 3854. (g) Khusnutdinova, J. R.; Newman, L. L.; Zavalij, P. Y.; Lam, Y. F.; Vedernikov, A. N. *J. Am. Chem. Soc.* **2008**, *130*, 2174. (h) Crespo, M.; Anderson, C. M.; Kfoury, N.; Font-Bardia, M.; Calvet, T. *Organometallics* **2012**, *31*, 4401. (i) Zhao, S. B.; Wang, R. Y.; Nguyen, H.; Becker, J. J.; Gagné, M. R. *Chem. Commun.* **2012**, *48*, 443. (j) Grice, K. A.; Kaminsky, W.; Goldberg, K. I. *Inorg. Chim. Acta* **2011**, *369*, 76.

(7) (a) Braunschweig, H.; Cogswell, P.; Schwab, K. *Coord. Chem. Rev.* **2011**, *255*, 101. (b) Sun, H. B.; Li, B.; Hua, R.; Yin, Y. *Eur. J. Org. Chem.* **2006**, 4231.

(8) (a) Nabavizadeh, S. M.; Habibzadeh, S.; Rashidi, M.; Puddephatt, R. J. *Organometallics* **2010**, *29*, 6359. (b) Jamali, S.; Nabavizadeh, S.

M.; Rashidi, M. *Inorg. Chem.* **2008**, *47*, 5441. (c) Aseman, M. D.; Rashidi, M.; Nabavizadeh, S. M.; Puddephatt, R. J. *Organometallics* **2013**, *32*, 2593−2598. (d) Nabavizadeh, S. M.; Shahsavari, H. R.; Sepehrpour, H.; Hosseini, F. N.; Jamali, S.; Rashidi, M. *Dalton Trans.* **2010**, *39*, 7800. (e) Nabavizadeh, S. M.; Amini, H.; Rashidi, M.; Pellarin, K. R.; McCready, M. S.; Cooper, B. F. T.; Puddephatt, R. J. *J. Organomet. Chem.* **2012**, *713*, 60. (f) Hoseini, S. J.; Nasrabadi, H.; Nabavizadeh, S. M.; Rashidi, M.; Puddephatt, R. J. *Organometallics* **2012**, *31*, 2357. (g) Nabavizadeh, S. M.; Aseman, M. D.; Ghaffari, B.; Rashidi, M.; Hosseini, F. N.; Azimi, G. *J. Organomet. Chem.* **2012**, *715*, 73. (h) Nabavizadeh, S. M.; Sepehrpour, H.; Shahsavari, H. R.; Rashidi, M. *New J. Chem.* **2012**, *36*, 1739. (i) Rashidi, M.; Nabavizadeh, S. M.; Akbari, A.; Habibzadeh, S. *Organometallics* **2005**, *24*, 2528.

(9) (a) Appleton, T. G.; Bennett, M. A.; Tomkins, I. B. *J. Chem. Soc., Dalton Trans.* **1976**, 439. (b) Cooper, S. J.; Brown, M. P.; Puddephatt, R. J. *Inorg. Chem.* **1981**, *20*, 1374.

(10) Smith, D. C., Jr.; Haar, C. M.; Stevens, E. D.; Nolan, S. P.; Marshall, W. J.; Moloy, K. G. *Organometallics* **2000**, *19*, 1427.

(11) (a) Romeo, R.; D'Amico, G. *Organometallics* **2006**, *25*, 3435. (b) Belluco, U.; Bertani, R.; Coppetti, S.; Michelin, R. A.; Mozzon, M. *Inorg. Chim. Acta* **2003**, *343*, 329.

(12) Momeni, B. Z.; Kazmi, H.; Najafi, A. *Helv. Chim. Acta* **2011**, *94*, 1618.

(13) Jain, V. K.; Jain, L. *Coord. Chem. Rev.* **2005**, *249*, 3075.

(14) Benjamin, S. L.; Levason, W.; Reid, G.; Rogers, M. C.; Warr, R. P. *J. Organomet. Chem.* **2012**, *708*, 106.

(15) Frisch, M. J.; Rega, N.; Petersson, G. A.; Trucks, G. W.; Nakatsuji, H.; Hada, M.; Ehara, M.; Toyota, K.; Fukuda, R.; Hasegawa, J.; Ishida, M.; Burant, J. C.; Nakajima, T.; Honda, Y.; Kitao, O.; Schlegel, H. B.; Nakai, H.; Klene, M.; Li, X.; Knox, J. E.; Hratchian, H. P.; Cross, J. B.; Millam, J. M.; Bakken, V.; Adamo, C.; Jaramillo, J.; Gomperts, R.; Scuseria, G. E.; Stratmann, R. E.; Yazyev, O.; Austin, A. J.; Cammi, R.; Pomelli, C.; Iyengar, S. S.; Ochterski, J. W.; Ayala, P. Y.; Morokuma, K.; Voth, G. A.; Salvador, P.; Robb, M. A.; Dannenberg, J. J.; Zakrzewski, V. G.; Dapprich, S.; Daniels, A. D.; Tomasi, J.; Strain, M. C.; Farkas, O.; Malick, D. K.; Rabuck, A. D.; Raghavachari, K.; Foresman, J. B.; Cheeseman, J. R.; Ortiz, J. V.; Cui, Q.; Baboul, A. G.; Barone, V.; Clifford, S.; Cioslowski, J.; Stefanov, B. B.; Liu, G.; Liashenko, A.; Piskorz, P.; Komaromi, I.; Montgomery Jr, J. A.; Martin, R. L.; Fox, D. J.; Mennucci, B.; Keith, T.; Al-Laham, M. A.; Peng, C. Y.; Nanayakkara, A.; Challacombe, M.; Gill, P. M. W.; Johnson, B.; Chen, W.; Vreven, T.; Wong, M. W.; Cossi, M.; Gonzalez, C.; Pople, J. A.; Kudin, K. N.; Scalmani, G. *Gaussian 03*, Revision C.02; Gaussian, Inc.: Wallingford, CT, 2004.

(16) (a) Hay, P. J.; Wadt, W. R. *J. Chem. Phys.* **1985**, *82*, 270. (b) Wadt, W. R.; Hay, P. J. *J. Chem. Phys.* **1985**, *82*, 284.

(17) *Chemissian V3.3*; http://www.chemissian.com

(18) The change in the Pt coordination (from four coordinate to five coordinate) has led to a minor change in phosphorus NMR. Note that a similar minor change has been observed in a four coordinate cycloplatinated(II) versus the five coordinated analogoue; see Frezza, M.; Dou, Q. P.; Xiao, Y.; Samouei, H.; Rashidi, M.; Samari, F.; Hemmateenejad, B. *J. Med. Chem.* **2011**, *54*, 6166.

(19) Zhu, J.; Lin, Z.; Marder, T. B. *Inorg. Chem.* **2005**, *44*, 9384.

(20) (a) Niroomand Hosseini, F.; Ariafard, A.; Rashidi, M.; Azimi, G.; Nabavizadeh, S. M. *J. Organomet. Chem.* **2011**, *696*, 3351. (b) Ariafard, A.; Ejehi, Z.; Sadrara, H.; Mehrabi, T.; Etaati, S.; Moradzadeh, A.; Moshtaghi, M.; Nosrati, H.; Brookes, N. J.; Yates, B. F. *Organometallics* **2011**, *30*, 422.